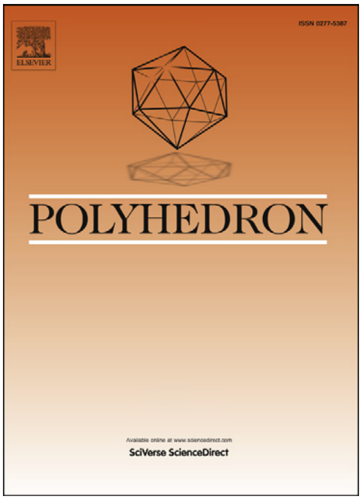

Self-Assembly of a Pentanuclear $\{Cu_5\}$ Complex Resulting from the Trapping of a Cu^{2+} Ion by Two $\{Cu_2\}$ Building Units

Aloke Kumar Ghosh, Rodolphe Clérac, Corine Mathonière, Debashis Ray

PII: S0277-5387(13)00153-8
DOI: http://dx.doi.org/10.1016/j.poly.2013.02.051
Reference: POLY 9960

To appear in: *Polyhedron*

Received Date: 9 January 2013
Accepted Date: 15 February 2013

Please cite this article as: A.K. Ghosh, R. Clérac, C. Mathonière, D. Ray, Self-Assembly of a Pentanuclear $\{Cu_5\}$ Complex Resulting from the Trapping of a Cu^{2+} Ion by Two $\{Cu_2\}$ Building Units, *Polyhedron* (2013), doi: http://dx.doi.org/10.1016/j.poly.2013.02.051

Self-Assembly of a Pentanuclear {Cu_5} Complex Resulting from the Trapping of a Cu^{2+} Ion by Two {Cu_2} Building Units

Aloke Kumar Ghosh,[a] Rodolphe Clérac,[b,c] Corine Mathonière[d,e] and Debashis Ray*[a]

[a] Department of Chemistry, Indian Institute of Technology, Kharagpur 721 302, India
Fax: (+91) 3222-82252; Tel: (+91) 3222-283324; E-mail: dray@chem.iitkgp.ernet.in
[b] CNRS, CRPP, UPR 8641, Pessac, F-33600, France.
[c] Univ. Bordeaux, CRPP, UPR 8641, Pessac, F-33600, France.
[d] CNRS, UPR 9048, ICMCB, Pessac, F-33600, France
[e] Univ. Bordeaux, ICMCB, UPR 9048, Pessac, F-33600, France.

Abstract

The compound $[Cu_5(\mu_3\text{-}OH)_2(H_2bpmp)_2(\mu_{1,1}\text{-}OAc)_2(\mu_{1,1,3}\text{-}OAc)_2(OAc)_2]\cdot 2H_2O$ ($1\cdot 2H_2O$) (H_3bpmp = 2,6-bis-[(3-hydroxy-propylimino)-methyl]-4-methyl-phenol), featuring two fused defective cubanes at a Cu^{2+} vertex, has been obtained *via* μ_3-OH-bridge-driven self-assembly of two dinuclear Cu(II) phenoxido-bridged {$Cu_2(H_2bpmp)$} fragments. Antiferromagnetic interactions within the complex lead to an $S_T = ½$ ground state for the pentanuclear arrangement.

Keywords. Self-assembly / pentanuclear / trapping / Schiff base / hydroxido and acetato bridges / antiferromagnetic interactions

1. Introduction

In recent years, high-nuclearity coordination complexes have attracted major interest in the areas of both synthetic chemistry and molecular magnetism [1,2]. The synthetic strategy involving the self-assembly processes of dinuclear {Cu_2} building blocks around a central oxido or metal ion and appropriate bridging/blocking ligands is a fascinating approach as the final outcome can never be totally predicted beforehand [3]. Because of the biological and biochemical importance of multicopper oxidase enzymes as dominant oxidizing agents toward different substrates in laccase [4,5], ascorbate oxidase and nitrite reductase [6], the understanding and synthetic control of the chemical aggregation of multi-copper coordination complexes is one of the major research areas in coordination chemistry [7]. Such coordination compounds are in general prepared *via* metal ion coordination driven self-assembly reactions with the use of suitable bridging and blocking ligands [8]. Among these Cu-based systems, the pentanuclear assembly with a 'vertex-shared defective dicubane' core is not commonly encountered [9]. In these {Cu_5} systems, the vertices are composed of either metal ions or oxygen donor atoms from oxido, hydroxido or acetato groups. Existing copper complexes involving all these three ligands as bridges and comprising multiple fused cubanes are extremely scarce [10a-d]. In this perspective, the reactivity of hexadenate/dinucleating phenolate Schiff base ligands like H_3bpmp (Chart 1, 2,6-bis-[(3-hydroxy-propylimino)-methyl]-4-methyl-phenol) with copper(II) in the presence of acetate anions have been explored. The use of the H_3bpmp ligand in transition-metal chemistry is relatively new, the only compound known is a dinuclear hydroxido-bridged copper(II) complex [11,12]. It is worth noting that use of two closely related ligands, Hbip and Hcip (Chart 1, R = benzyl; Hbip: 2,6-*bis*(benzyl imino methyl)-4-methylpheno and R = cyclohexyl; Hcip: 2,6-*bis*(cyclohexyl imino methylene)-4-methylphenol), led to interesting systems, consisting of {Cu_4} complexes, showing chemical reactivity and core conversion reactions [13,14].

Chart 1.

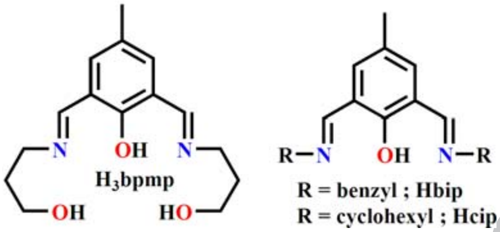

In this work, the coordinating and aggregating abilities of H_3bpmp (Scheme S1), together with the varying binding properties of acetate ions, have been exploited for the preparation of a novel pentanuclear complex, $[Cu_5(\mu_3\text{-}OH)_2(H_2bpmp)_2(\mu_{1,1}\text{-}OAc)_2(\mu_{1,1,3}\text{-}OAc)_2(OAc)_2]\cdot 2H_2O$ (**1**·$2H_2O$).

2. Experimental Section

2.1 Materials and Physical Methods.

The chemicals used were obtained from the following sources: copper(II) acetate monohydrate from S.D. Fine Chemicals, triethylamine from Merck, India and 3-amino-1-propanol from Aldrich Chemical Co. Inc. US. All other chemicals and solvents were reagent-grade materials and were used as received without further purification. 2,6-Diformyl-4-methylphenol (2-hydroxy-5-methyl-benzene-1,3-dicarbaldehyde) was prepared following a literature procedure [15]. The elemental analyses (C, H, N) were performed with a Perkin-Elmer model 240 C elemental analyzer. Fourier transform infrared (FTIR) spectra were recorded on a Perkin-Elmer RX1 spectrometer. Solution electrical conductivity measurements and electronic spectra were carried out using a Unitech type U131C digital conductivity meter with a solute concentration of about 10^{-3} M and a Shimadzu UV 3100 UV-vis-NIR spectrophotometer, respectively. The magnetic susceptibility measurements were obtained with the use of a Quantum Design SQUID magnetometer, MPMS-XL. This magnetometer works between 1.8 and 400 K for dc applied fields ranging from -7 to 7 T. Measurements were performed on microcrystalline samples of 22.13 mg for **1**·$2H_2O$. The magnetic data are corrected for the sample holder and the diamagnetic contributions.

2.2 Synthesis

H_3bpmp Ligand. The H_3bpmp Schiff-base ligand was prepared from the single step condensation of 2,6-diformyl-4-methylphenol (1.0 g, 6.1 mmol) and 3-amino-1-propanol (0.91 g, 12.2 mmol) in methanol (20 mL) in air at room temperature (28 °C), under stirring for 2 h. Complete evaporation of the solvent in air over 12 h yielded an orange colored semi-solid product which was used directly for the reaction without further characterization. Yield: 1.32g (78%).

$[Cu_5(\mu_3\text{-OH})_2(\mu\text{-bpmp})_2(\mu_{1,1}\text{-OAc})_2(\mu_{1,1,3}\text{-OAc})_2(OAc)_2]\cdot 2H_2O$.

A methanolic solution (10 mL) of $Cu(OAc)_2\cdot H_2O$ (0.599 g, 3.00 mmol) was slowly added to the H_3bpmp ligand (0.278 g, 1.00 mmol) in methanol (20 mL), followed by addition of NEt_3 (139 mL, 0.101 g, 1.00 mmol). The resulting solution was stirred for 2 h at room temperature. The solvent was evaporated in air to give a green solid that was isolated, washed with cold methanol and dried under vacuum over P_4O_{10}. Green crystals suitable for X-ray analysis were obtained from a MeOH solution after two weeks. Yield: 0.492 g, 76%. Anal. Calcd. for $C_{42}H_{66}Cu_5N_4O_{22}$

(1296.71 g mol^{-1}): C, 38.90; H, 5.13; N, 4.32. Found: C, 38.82; H, 5.22; N, 4.22. Selected FT-IR bands (KBr, cm^{-1}; s = strong, vs = very strong, m = medium, br = broad): 3387(br), 2926(s), 1638(s), 1578(s), 1396(vs), 1334(s), 1076(vs), 918(m), 681(m), Molar conductance, $_{\mathrm{M}}$ (MeOH solution, Ω^{-1} cm^2 mol^{-1}): 6.3. UV-vis spectra [$_{\mathrm{max}}$, nm (, L mol^{-1} cm^{-1})] (MeOH solution) : 666 (235), 370 (5120), 210 (17700).

2.3 X-ray crystallography

The diffraction data of the complex **1**·2H_2O was collected on a Bruker APEX-II CCD X-ray diffractometer using single crystals, with graphite-monochromated Mo-K_α radiation (λ = 0.71073 Å) by the -scan method at 293 K. Information concerning X-ray data collection and structure refinement of the compound is summarized in Table 1. For complex **1**·2H_2O, a total of 7960 reflections were recorded with Miller indices h_{min} = -16, h_{max} = 16, k_{min} = -19, k_{max} = 20, l_{min} = -23, l_{max} = 22 .In the final cycles of full-matrix least squares on F^2, all non-hydrogen atoms were assigned anisotropically. The structure was solved using the SHELX-97 [16] program system.

Table 1. Crystallographic data for **1**·2H_2O

compound	**1**·2H_2O
formula	$C_{42}H_{66}Cu_5N_4O_{22}$
M	1296.71
space group	*P* 2_1/c
crystal system	monoclinic
a/Å	11.4604(7)
b/Å	13.7598(8)
c/Å	17.3334(10)
β/deg	103.317(2)

$V/Å^3$	2659.85(3)
T/K	293
Z	3
D_c/g cm^{-3}	1.619
F(000)	1334
crystal size/mm	0.36 x 0.25 x 0.15
μ(Mo-Kα)/cm^{-1}	20.47
measured Refl.ns	39472
unique Ref.ns	7960
R_{int}	0.0377
obs. refl.ns $I \geq 2\sigma(I)$	5671
θ_{min}- θ_{max}/°	1.83 -31.86
hkl ranges	-16, 16;-19, 20; -23,22
R(F^2) (obs.refl.ns)	0.0367
wR(F^2) (all refl.ns)	0.1009
no. variables	347
GOF	1.026
$\Delta\rho_{max}$; $\Delta\rho_{min}$ (e $Å^{-3}$)	0.621; -0.481

$R_1 = (\quad F_o \quad F_c \quad)/ \quad F_o$. $wR_2 = [\; w(F_o \quad F_c)^2/ \; w(F_o)^2]^{1/2}$. $w = 0.75/(\; ^2(F_o) +0.0010F_o^2)$.

3. Results and Discussion

3.1 Synthetic Considerations. H_3bpmp was prepared (Scheme S2 in the Supporting Information) following a reported procedure, [17] and its reactions with copper(II) salts have been investigated (Scheme 1). The reaction of $Cu(OAc)_2 \cdot H_2O$ with H_3bpmp in MeOH and NEt_3 gave $[Cu_5(\mu\text{-}H_2bpmp)_2(\mu_3\text{-}OH)_2(\mu_{1,1}\text{-}OAc)_2(\mu_{1,1,3}\text{-}OAc)_2(OAc)_2] \cdot 2H_2O$. Complex **1**$\cdot 2H_2O$ was obtained as a precipitate in 76% yield from MeOH, as summarized in eq. 1, clearly accounting for the formation the two hydroxido bridges from water molecules present in the organic solvent medium. The elemental analysis, molar conductivity and single-crystal X-ray diffraction (*vide* *infra*) data confirm the given formula $[Cu_5(\mu\text{-}H_2bpmp)_2(\mu_3\text{-}OH)_2(\mu_{1,1}\text{-}OAc)_2(\mu_{1,1,3}\text{-}OAc)_2(OAc)_2]$ for **1**.

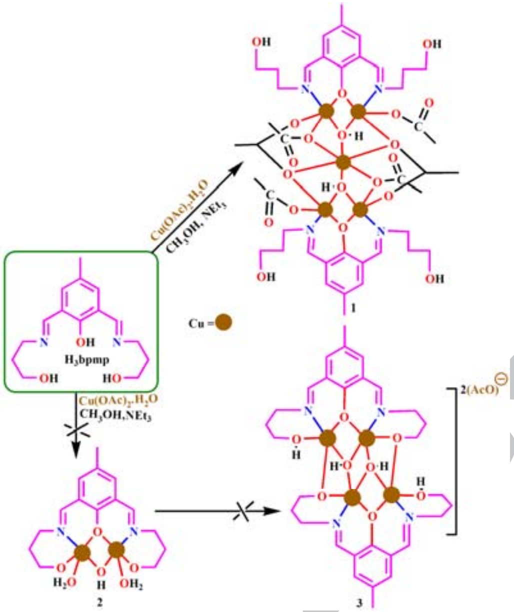

Scheme 1. Schematic representation of the non-formation of {Cu2} and {Cu4}, and formation of $\{Cu_5\}$ assemblies

$$4H_3bpmp + 5Cu_2(OAc)_4\cdot 2H_2O + 8NEt_3 \longrightarrow 2[Cu_5(\mu\text{-}H_2bpmp)_2(\mu_3\text{-}OH)_2(\mu_{1,1}\text{-}OAc)_2(\mu_{1,1,3}\text{-}OAc)_2(OAc)_2]\cdot 2H_2O + 8(HNEt_3)(OAc) + 2H_2O \quad \cdots (1)$$

The vertex-shared $\{Cu_5\}$complex **1** results from the binding of two μ-H_2bpmp ligands in front of a Cu^{II}/AcO system, as opposed to tetranuclear or dinuclear complexes (Scheme 1).

3.2 Description of the Crystal Structure. The crystallographic asymmetric unit consists of one-half of the pentanuclear unit and one interstitial solvent H_2O molecule. The second half of the complex is generated from the above mentioned unit by symmetry operations (-x, 1-y, -z). Complex **1** is a centrosymmetric pentanuclear Cu^{II} species formed of two defective cubanes around the central Cu^{II}, with a $[Cu_5O_{10}]$ core (Figures 1 and S1-S4). Important bond lengths and

Table 2. Selected inter-atomic distances (Å) and angles (º) for the complex **1**·$2H_2O$

Distances			
O(3)-Cu(2)	1.925(1)	Cu(2)-N(1)	1.953(2)
O(4)-Cu(1)	2.253(1)	Cu(2)-O(1)	1.970(1)
Cu(1)-O(2)	1.981(1)	Cu(2)-O(6)*	2.376(1)
Cu(1)-O(2)*	1.981(1)	Cu(2)-Cu(3)	3.058(4)
Cu(1)-O(6)	2.009(1)	Cu(3)-O(2)	1.930(1)
Cu(1)-O(6)*	2.009(1)	Cu(3)-O(8)	1.935(1)
Cu(1)-O(4)*	2.253(1)	Cu(3)-N(2)	1.941(2)
Cu(1)-Cu(2)	2.969(3)	Cu(3)-O(1)	1.984(1)
Cu(1)-Cu(2)*	2.969(3)	O(6)-Cu(2)	2.376(1)
Cu(2)-O(2)	1.9325(1)		
Angles			
O(2)-Cu(1)-O(2)*	180.0	O(2)-Cu(2)-N(1)	170.4(7)
O(2)-Cu(1)-O(6)*	87.1(7)	O(3)-Cu(2)-O(1)	166.3(7)
O(2)*-Cu(1)-O(6)*	92.8(7)	O(2)-Cu(2)-O(1)	77.1(6)
O(2)*-Cu(1)-O(6)	92.8(7)	N(1)-Cu(2)-O(1)	93.3(7)
O(2)*-Cu(1)-O(6)	87.1(7)	O(3)-Cu(2)-O(6)*	102.2(7)
O(6)-Cu(1)-O(6)*	180.0	O(2)-Cu(2)-O(6)*	78.6(6)
O(2)-Cu(1)-O(4)*	88.8(6)	N(1)-Cu(2)-O(6)*	100.3(7)
O(2)-Cu(1)-O(4)	91.1(6)	O(1)-Cu(2)-O(6)*	86.0(6)
O(6)*-Cu(1)-O(4)*	87.3(7)	O(3)-Cu(2)-Cu(1)	84.7(5)
O(6)*-Cu(1)-O(4)	92.6(7)	O(2)-Cu(2)-Cu(1)	41.2(5)
O(2)-Cu(1)-O(4)	91.1(6)	N(1)-Cu(2)-Cu(1)	140.9(6)
O(2)*-Cu(1)-O(4)	88.8(6)	O(1)-Cu(2)-Cu(1)	94.5(4)
O(6)*-Cu(1)-O(4)	92.6(7)	O(6)*-Cu(2)-Cu(1)	42.3(4)
O(6)*-Cu(1)-O(4)*	87.3(7)	O(3)-Cu(2)-Cu(3)	130.5(5)
O(4)*-Cu(1)-O(4)	180.0	O(2)-Cu(2)-Cu(3)	37.6(5)
O(2)-Cu(1)-Cu(2)	40.0(5)	N(1)-Cu(2)-Cu(3)	132.8(6)
O(2)-Cu(1)-Cu(2)*	139.9(5)	O(1)-Cu(2)-Cu(3)	39.5(4)
O(6)*-Cu(1)-Cu(2)	52.8(4)	O(6)*-Cu(2)-Cu(3)	80.2(4)
O(6)*-Cu(1)-Cu(2)*	127.1(4)	Cu(1)-Cu(2)-Cu(3)	63.9(7)
O(4)-Cu(1)-Cu(2)*	105.2(4)	O(2)-Cu(3)-O(8)	94.6(7)
O(4)-Cu(1)-Cu(2)	74.7(4)	O(2)-Cu(3)-N(2)	167.4(8)
O(2)*-Cu(1)-Cu(2)	139.9(5)	O(8)-Cu(3)-N(2)	97.1(8)
O(2)*-Cu(1)-Cu(2)*	40.0(5)	O(2)-Cu(3)-O(1)	76.8(6)
O(6)-Cu(1)-Cu(2)	127.1(4)	O(8)-Cu(3)-O(1)	167.2(7)
O(6)-Cu(1)-Cu(2)*	52.8(4)	N(2)-Cu(3)-O(1)	92.1(7)

O(4)-Cu(1)-Cu(2)	74.7(4)	O(2)-Cu(3)-Cu(2)	37.6(5)
O(4)*-Cu(1)-Cu(2)	105.2(4)	O(8)-Cu(3)-Cu(2)	131.6(5)
Cu(2)-Cu(1)-Cu(2)*	180.0	N(2)-Cu(3)-Cu(2)	131.0(6)
O(3)-Cu(2)-O(2)	93.6(7)	O(1)-Cu(3)-Cu(2)	39.1(4)
O(3)-Cu(2)-N(1)	95.8(7)	Cu(3)-O(2)-Cu(2)	104.6(8)
Cu(3)-O(2)-Cu(1)	109.3(8)	Cu(2)-O(2)-Cu(1)	98.6(7)
*: -x, 1-y,- z			

angles are listed in Table 2, where the bridges between the metal ions are ensured by two water derived μ_3-OH anions, four acetato ligands (two each in $\mu_{1,1,3}$, $\mu_{1,1}$ modes) and two μ-phenoxido moieties from deprotonated H_2bpmp ligands.

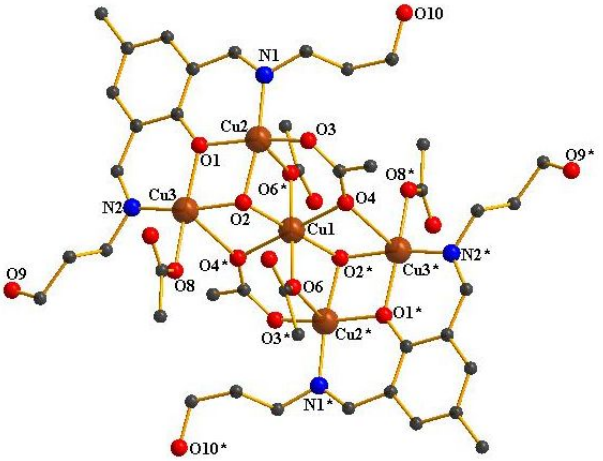

Figure 1. View of the pentanuclear unit of [$Cu_5(\mu$-H_2bpmp$)_2(\mu_3$-$OH)_2(\mu_{1,1}$-$OAc)_2(\mu_{1,1,3}$-$OAc)_2(OAc)_2]\cdot 2H_2O$ in **1**$\cdot 2H_2O$

The central Cu(1) adopts an *octahedral* coordination sphere with an O_6 donor environment made from the coordination of hydroxido (O(2)) and acetate (O(4) and O(6)) groups, having long Cu(1)-O(4) *apical* bonds (2.253 Å) as expected from a Jahn-Teller distortion along the *z* axis. (Figure S5). The remaining coordination sites of the *square pyramidal* Cu^{II} ions (Addison [18] τ

values 0.06 and 0.003) are completed by peripheral imine groups from H_2bpmp ligands. Interestingly, both the alcohol arms of the ligand H_2bpmp remain uncoordinated and one of them is engaged in inter-molecular hydrogen-bonding interactions with water molecules of crystallization (Figure S6). The other uncoordinated arms show intra-molecular hydrogen-bonding interactions with free carbonyl oxygen atoms of bridging $\mu_{1,1}$ acetate groups. There are all together three different types of acetate groups present in the compound (Figure S7). The affinity of the copper(II) ions for long distance binding along the *apical* Jahn-Teller axis is responsible for the binding of six AcO ions in these three different modes. Inspection of Figure 1 suggests that the formation of **1** occurs through the trapping of an $[Cu(OAc)_2(H_2O)_2]$ species by two hitherto unknown $\{Cu_2\}$ fragments, $[Cu_2(\mu\text{-}H_2bpmp)_2(\mu\text{-}OH)(OAc)_2]$. During this assembly, the double hydroxido bridge of the $\{Cu_2\}$ fragments extends its binding capacity to μ_3-OH and one of the acetato group to $\mu_{1,1}$-OAc. The trapped acetato groups of $[Cu(OAc)_2(H_2O)_2]$ are converted to the $\mu_{1,1}$ mode and one acetato group on each metal ion of the $\{Cu_2\}$ fragments is transformed to the $\mu_{1,1,3}$ mode. Three different types of acetato ligands in $\mu_{1,1,3}$, $\mu_{1,1}$ and monodentate binding modes stabilize the coordination complex by satisfying the geometry and coordination demands of the copper(II) centers. These three different types of AcO binding modes in a single acetate rich complex are rather exceptional. The two hydroxido bridges have the primary control on the formation of the $\{Cu_5\}$ entity, like that observed in the copper-based minerals shattuckite, $Cu_5(OH)_2(SiO_3)_4$, cornubite, $Cu_5(OH)_2(AsO_4)_2$ and chloride in the place of hydroxide in the copper selenite chloride compound, $Cu_5Cl_2(SeO_3)_4$ [19a,b]. The five Cu^{II} atoms of the complex are at five vertices of a 'vertex shared opened-dicubane' [20], where one vertex of each cubane is missing and the octahedral copper(II) center occupies a mutual vertex of each opened-cubane (Figure S8).

3.3 FT-IR Spectroscopy. The presence of lattice uncoordinated alcohol groups, lattice water molecules and hydroxido ligands in **1** is manifested by one broad band of medium intensity at 3387 cm^{-1}, assigned to $\bar{\nu}$(OH). The broadness and relatively low frequency are both indicative of hydrogen bonding. Several bands for **1** also appear in the 1638 1396 cm^{-1} region for this complex. Contributions from $\bar{\nu}$(C=N), (OH), $\bar{\nu}_{as}$(COO) and $\bar{\nu}_{s}$(COO) are expected in this region for three different types of acetato coordination, but overlap with the stretching vibrations of the aromatic ring of the ligand occasionally renders the assignments and discussion of the shifts of the stretching frequencies during coordination difficult. The $\bar{\nu}_{C=N}$ stretching frequency is observed at 1638 cm^{-1} for complex **1**. The bands at 1578 and 1396 cm^{-1} in the spectrum of **1** are tentatively assigned to the $\bar{\nu}_{as}$(COO) and $\bar{\nu}_{s}$(COO) carboxylate modes, respectively. The parameter , where = $\bar{\nu}_{as}$(COO) $\bar{\nu}_{s}$(COO), is 182 cm^{-1} as expected for the $\mu_{1,1,3}$-bridging mode of the acetate ligation [20]. As noted earlier, the bands assignable to $\mu_{1,1}$-bridging and non-bridging modes are difficult to assign in this range.

3.4 Electronic UV-Vis Spectra. Complex **1** in MeOH solution shows multiple bands in the 900-200 nm region. A broad absorption band (λ), with a maximum at 666 nm (ε = 235 L $mol^{-1}cm^{-1}$) for **1**, is due to a d-d transition, available for copper(II) bound to the H_3bpmp ligand. A shoulder at 370 nm (ε = 5120 L $mol^{-1}cm^{-1}$), for this complex is possibly due to HO^- Cu^{II} and PhO^- Cu^{II}

ligand-to-metal charge transfer (LMCT) transitions [21]. The intense absorption at 210 nm (ε = 17700 L mol^{-1}cm^{-1}) for **1** is from intraligand π π * transitions.

3.5 Magnetic Properties: The solid-state magnetic properties of **1**·2H$_2$O were investigated using dc susceptibility measurements in the 1.8-300 K temperature range under a magnetic field of 1 T. At room temperature, the χT product is 0.89 cm^3 K mol^{-1}. This χT value is far from the theoretical value of 1.875 cm^3 K mol^{-1} expected for five isolated paramagnetic Cu^{2+} ions (d^9, S = ½) with g = 2, indicating that strong and dominant antiferromagnetic interactions exist between the Cu^{2+} ions in the complex. Upon cooling, the χT product continuously decreases to reach a value close to 0.47 below 70 K. Using the structure of **1** as a guide, the complex can be viewed as an assembly of dinuclear units, each formed by the two external Cu(II) ions, linked together by a central Cu(II) ion. The bridging geometry in the dinuclear units is made of one μ-phenoxido and one μ_3-hydroxido group, with Cu(2)-O(2)-Cu(3) and Cu(2)-O(1)-Cu(3) angles of 104.69 and 101.31°, respectively (Figure 2).

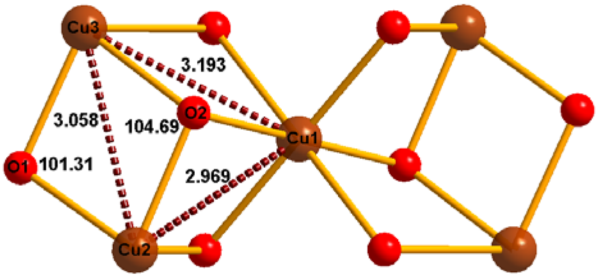

Figure 2. The metallic core of **1**·2H$_2$O

Generally speaking for the Cu^{II} ions, the magnetic interactions mediated through their *apical* positions are much weaker than those mediated by their *basal* sites. Therefore, if one considers only the magnetic pathways that involve *basal* bonds around each Cu^{II} ion, **1** can be viewed as the sum of two dinuclear units linked by a central Cu^{II} ion. As a consequence, the complex can be topologically viewed as two spin dimers composed of two S = ½ Cu^{II} ions and one isolated S = ½ spin (the central Cu^{II} ion). As a first approximation, the magnetic data were modelled using an isotropic spin Heisenberg Hamiltonian to estimate the value of the exchange interaction in each dimmer, as given in eq. 2.

$$H = -2J\left\{S_{Cu,1} \bullet S_{Cu,2}\right\} \qquad (2)$$

where, J is the exchange interaction within the dinuclear Cu(II) units; $\boldsymbol{S}_\mathrm{i}$ the spin operators for each center with S = ½. The application of the van Vleck equation [22,23] allows the determination of the low field analytical expression of the magnetic susceptibility, including the Curie component of the central Cu(II) spin, as given in eq. 3 [24].

$$\chi T = 2\times\frac{2N\mu_B^2 g_{Cu2,3}^2}{k_B}\frac{1}{3+\exp\left(-2J/k_B T\right)}+\frac{N\mu_B^2 g_{Cu1}^2}{4k_B} \qquad (3)$$

As shown in Figure 3, this model reproduces the experimental χT *vs*. T data very well with the best set of parameters being $g_{Cu2,3}$= 2.16(5) (the Zeeman factor of the Cu^{II} ions in the dimer units), g_{Cu1} = 2.24(5) (the Zeeman factor of the central Cu^{II} ion) and J/k_B = -400(3) K.

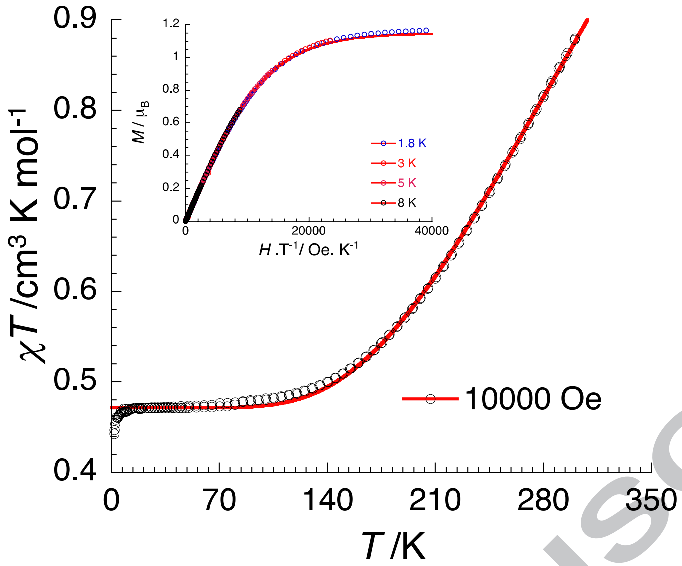

Figure 3. Temperature dependence of the T product (being the molar magnetic susceptibility defined as M/H) at 1 T for **1**·2H_2O. The solid line is the best fit obtained using the isotropic dinuclear S = ½ Heisenberg model described in the text. Inset: Field dependence of the magnetization at 1.8, 3, 5 and 7 K plotted as M *vs.* H/T. The solid lines are the best fits obtained with the S = ½ Brillouin function.

The sign of the magnetic interactions implies that the two dinuclear Cu units possess an $S_T = 0$ spin ground state. It is worth mentioning that this fit, with a single intramolecular magnetic interaction (the interaction between the external and central Cu(II) centers being negligible), works remarkably well and therefore it is not reasonable to add into the model the second (much weaker) intra-molecular magnetic interaction involving the central Cu^{II} ion without facing over parametrization and multiple solutions. The field dependence of the magnetization in the 1.8-8 K range was also measured. These data shows that the magnetization at 1.8 K under 7 T is saturated at 1.16 μ_B, as expected for one isolated S = ½ spin born by the central Cu^{II} ion with a g factor higher than 2. The M *vs* H/T data can be fitted relatively well to an S = ½ Brillouin function with a *g* value of 2.30(5), corresponding to the g_{Cu1} value obtained from the χT *vs* T data.

4. Conclusion. In summary, a new pentanuclear {Cu_5} complex, **1**, has been synthesized by the combined action of AcO and HO anions, together with the H_3bpmp Schiff base ligand. This aggregate possesses a geometry that can be described as double defective cubanes sharing a central Cu(II) vertex that is stabilized by a set of bridging acetates in $\mu_{1,1}$ and $\mu_{1,1,3}$-modes, two hydroxides in the μ_3-mode and phenoxido groups in a normal two centered bridging mode. These bridges mediate within the pentanuclear complex **1**, dominating antiferromagnetic interactions, inducing an $S_T = ½$ spin ground state. This work emphasizes the role of acetate ligands for the self-assembly of two H_2bpmp^- ligated {Cu_2} fragments, which are responsible for the trapping of the central Cu^{2+} ion.

Acknowledgements. A.K.G. is thankful to the Council of Scientific and Industrial Research, New Delhi, India for financial support. C.M. acknowledges the Institut Universitaire de France (IUF) for financial support. R.C. and C.M. acknowledge the University of Bordeaux, Région Aquitaine, GIS Advanced Materials in Aquitaine (COMET Project) and the CNRS for financial support.

Appendix A. Supporting information. CCDC 832928 contains the supplementary crystallographic data for **1**·$2H_2O$. The data can be obtained free of charge from www.ccdc.cam.ac.uk/conts/retrieving.html or from the Cambridge Crystallographic Data Centre, 12 Union Road, Cambridge CB2 1EZ, U.K.; fax, +44-1223/336-033; e-mail, deposit@ccdc.cam.ac.uk. Supplementary data associated with this article can be found, in the online version.

References

[1] E. C. Yang, D. Ding, Z. Y. Liu, Y. L. Yang, X. J. Zhao, Cryst. Growth Des. 12 (2012) 1185-1192.

[2] E. E. Moushi, C. Lampropoulos, W. Wernsdorfer, V. Nastopoulos, G. Christou, A. J. Tasiopoulos, J. Am. Chem. Soc.132 (2010) 16146-16155.

[3] R. E. P. Winpenny, J. Chem. Soc., Dalton Trans. (2002) 1-10.

[4] E. I. Solomon, U. M. Sundaram, T. E. Machonkin, Chem. Rev. 96 (1996) 2563-2606.

[5] M. Alcalde, J. Polaina, A.P. MacCabe (eds.), Industrial Enzymes. 2007, pp. 461-476.

[6] M. Kumar, N. A. Dixon, A. C. Merkle, M. Zeller, N. Lehnert, E. T. Papish, Inorg. Chem. 51 (2012) 7004-7006.

[7] X. M. Zhang, J. Lv, F. Ji, H. S. Wu, H. Jiao, P. v. R. Schleyer, J. Am. Chem. Soc. 133 (2011) 4788-4790.

[8] S. Ali, C. A. Muryn, F. Tuna, R. E. P. Winpenny, Dalton Trans. 39 (2010) 124-131.

[9] Y. Ma, Y. Q. Wen, J. Y. Zhang, E. Q. Gao, C. M. Liu, Dalton Trans. 39 (2010) 1846-1854.

[10] (a) S. Majumder, S. Sarkar, S. Sasmal, E. C. Sañudo, S. Mohanta, Inorg. Chem. 50 (2011) 7540-7554. (b) K. Dhara, J. Ratha, M. Manassero, X-Y. Wang, S. Gao, P. Banerjee, J. Inorg. Biochem. 101 (2007) 95-103. (c) C. P. Pradeep, S. Supriya, P. S. Zacharias, S. K. Das. Polyhedron. 25 (2006) 3588-3592. (d) Z-B. Han, G-X. Zhang, M-H. Zeng, D-Q. Yuan, Q-R. Fang, J-R. Li, J. Ribas, H-C. Zhou. Inorg. Chem. 49 (2010) 769-771.

[11] S. K. Mandal, K. Nag, J. Chem. Soc., Dalton. Trans. (1984) 2141-2149.

[12] A. Asokan, B. Varghese, P. T. Manoharan, Inorg. Chem. 38 (1999) 4393-4399.

[13] M. Sarkar, R. Clérac, C. Mathonière, N. G. R. Hearns, V. Bertolasi, D. Ray, Inorg. Chem. 49 (2010) 6575-6585.

[14] M. Sarkar, R. Clérac, C. Mathonière, N. G. R. Hearns, V. Bertolasi, D. Ray, Inorg. Chem. 50 (2011) 3922-3933.

[15] R. R. Gagne, C. L. Spiro, T. J. Smith, C. A. Hamann, W. R. Thies, A. K. Shiemke, J. Am. Chem. Soc. 103 (1981) 4073-4081.

[16] G. M. Sheldrick, SHELX-97, Program for Crystal Structure and Refinement, University of Göttingen, Germany, 1997.

[17] A. Sarkar, A. K. Ghosh, V. Bertolasi, D. Ray, Dalton Trans. 41 (2012) 1889-1895.

[18] W. A. Addison, T. N. Rao, J. Reedijk, J. V. Rijn, G. C. Verschoor, J. Chem., Soc. Dalton Trans. (1984) 1349-1356.

[19] (a) Z. Johan, J. H. Novakit, Chem. der. Erde. 20 (1958) 49-50.(b) D. Zhang, H. Berger, R. Kremer, D. Wulferding, P. Lemmens, M. Johnsson, Inorg. Chem. 49 (2010) 9683-9688.

[20] A. Escuer, G. Vlahopoulou, S. P. Perlepes, F. A. Mautner, Inorg. Chem. 50 (2011) 2468-2478.

[21] L. Lei, K. D. Karlin, S. E. Rokita, J. Am. Chem. Soc.127 **(**2005) 520-521.

[22] J. H. van Vleck, The Theory of Electric and Magnetic Susceptibility; Oxford University Press, 1932.

[23] K. Kambe, J. Phys. Soc. Jpn. 5 (1950) 48.

[24] C. J. O'Connor, Prog. Inorg. Chem. 29 (1982) 203-283.

Graphical Abstract

Self-Assembly of a Pentanuclear {Cu_5} Complex Resulting from the Trapping of a Cu^{2+} Ion by Two {Cu_2} Building Units

Aloke Kumar Ghosh,[a] Rodolphe Clérac,[b,c] Corine Mathonière,[d,e] and Debashis Ray*[a]

The binding of acetate anions in three different modes along with water derived μ_3-hydroxido groups dictate the stabilization of a pentanuclear copper(II) complex resulting from the self-assembly of two dinuclear {Cu_2} units around a central copper ion.

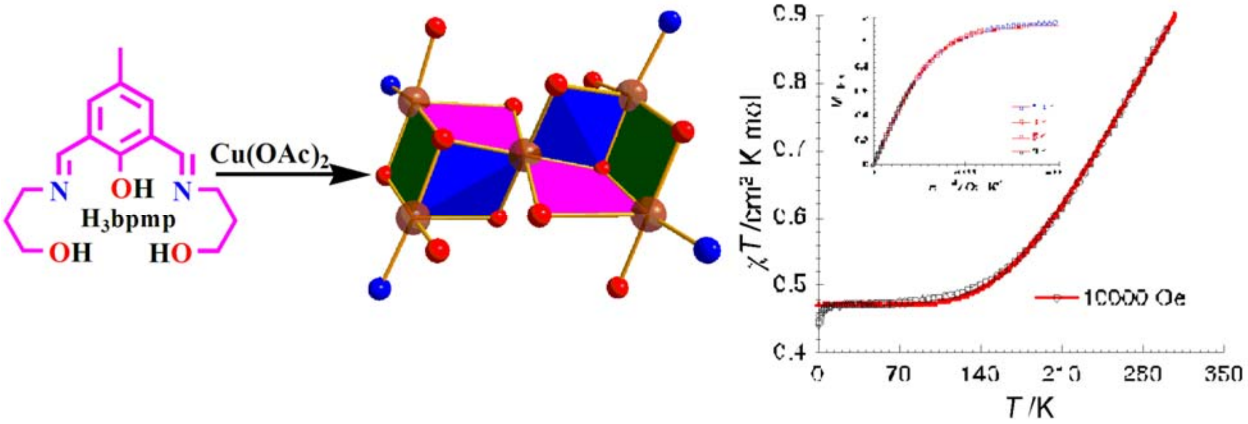

Supporting Information

Self-Assembly of a Pentanuclear {Cu_5} Complex Resulting from the Trapping of a Cu^{2+} Ion by Two {Cu_2} Building Units

Aloke Kumar Ghosh,[a] Rodolphe Clérac,[b,c] Corine Mathonière[d,e] and Debashis Ray*[a]

[a] Department of Chemistry, Indian Institute of Technology, Kharagpur 721 302, India

Fax: (+91) 3222-82252; Tel: (+91) 3222-283324; E-mail: dray@chem.iitkgp.ernet.in

[b] CNRS, CRPP, UPR 8641, Pessac, F-33600, France.

[c] Univ. Bordeaux, CRPP, UPR 8641, Pessac, F-33600, France.

[d] CNRS, UPR 9048, ICMCB, Pessac, F-33600, France

[e] Univ. Bordeaux, ICMCB, UPR 9048, Pessac, F-33600, France.

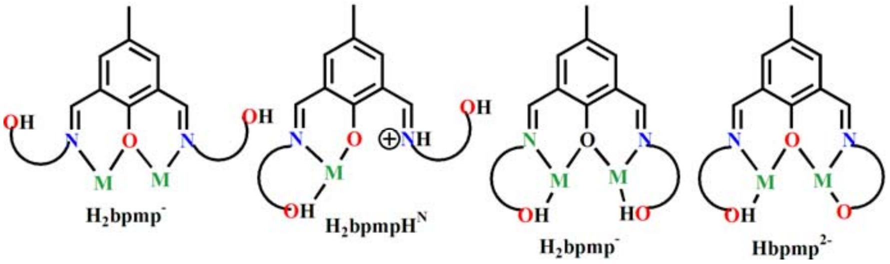

Scheme S1. Different binding modes of H_3bpmp

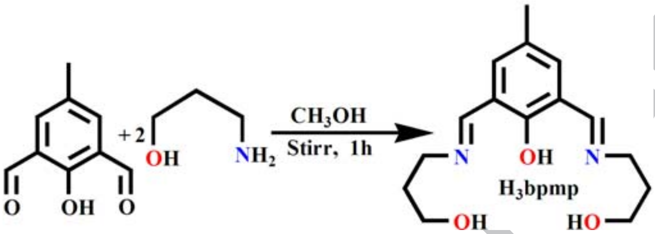

Scheme S2. Synthesis of the H_3bpmp ligand.

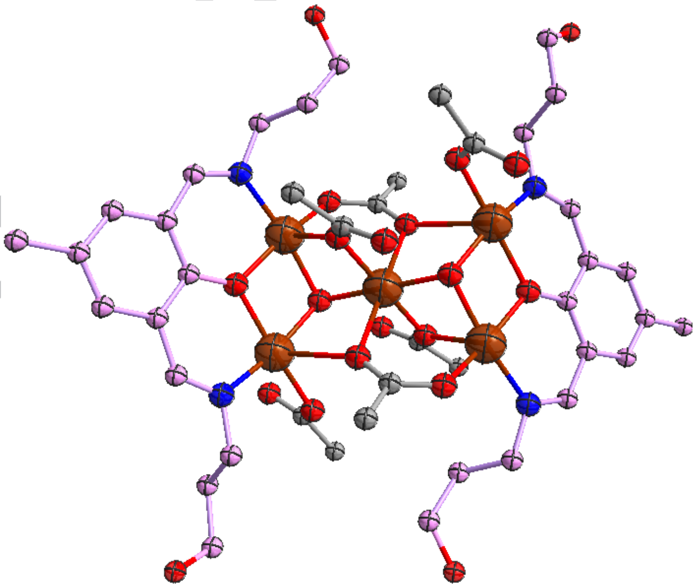

Figure S1. DIAMOND [1] view of $\mathbf{1}\cdot 2H_2O$ showing the ligand with different colors; red, O; blue, N; brown, Cu; pink, H_2bpmp (the thermal ellipsoids are shown at 40% probability).

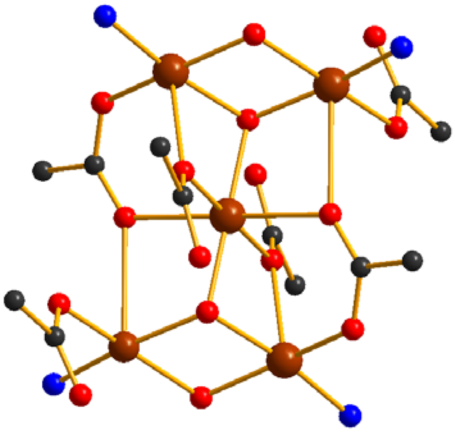

Figure S2. View of the atom connectivity within the [Cu_5] complex with three different types of acetato binding modes in **1**·$2H_2O$. Color code: brown, Cu; blue, N; red, O; black, C.

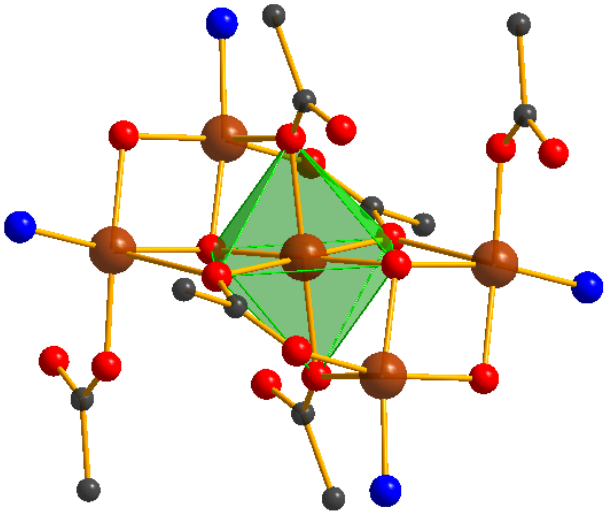

FigureS3. Molecular view of **1**·$2H_2O$ with the highlighted octahedral environment of the central copper atom.

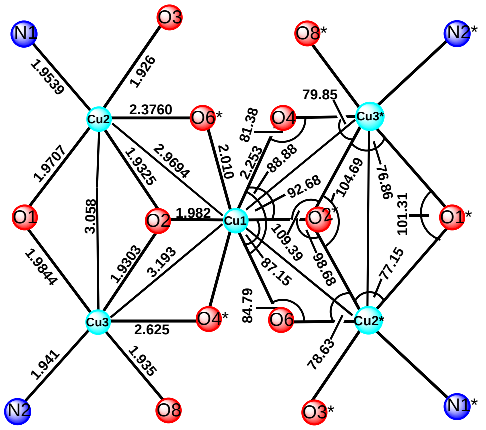

Figure S4. Atom connectivity of the pentanuclear Cu(II) core in **1**·$2H_2O$ with the relevant inter-atomic bond distances (Å) and angles (º). Atoms labelled with a '*' are generated from the parent atoms through the symmetry operation (-x, 1-y,- z).

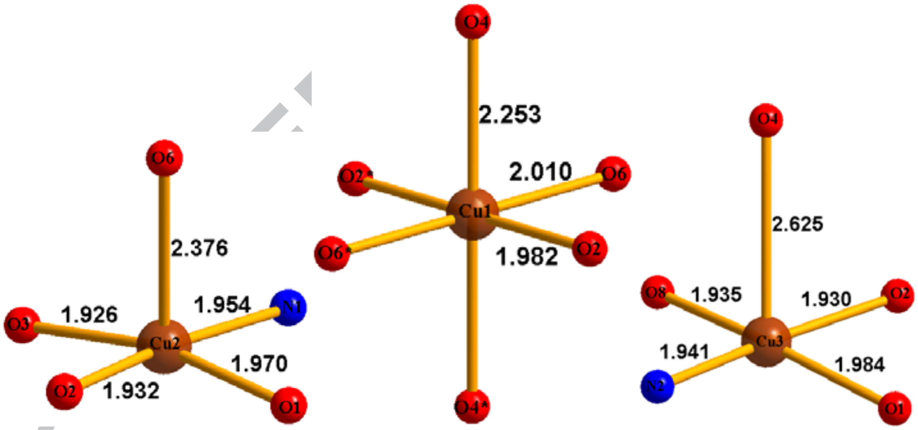

Figure S5. Geometry of the coordination sphere around the crystallographically independent copper(II) ions in complex **1**.

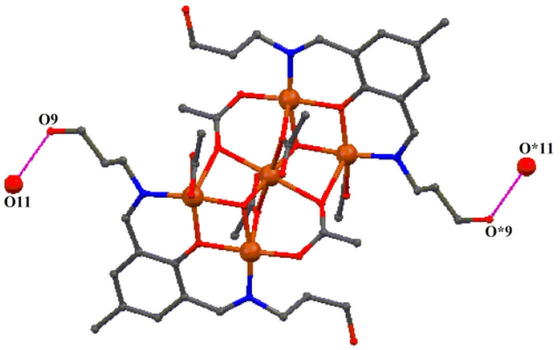

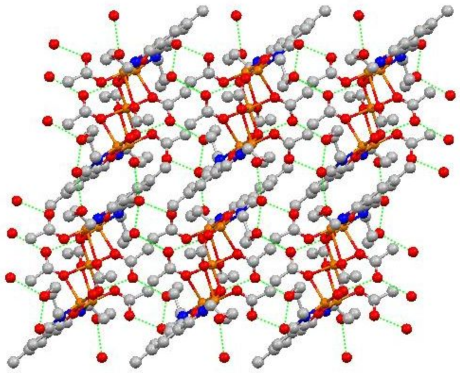

Figure S6. Ball and stick style representations of **1**·$2H_2O$ emphasizing the intra- and inter-molecular hydrogen bonds (labelled as pink lines) established around the [Cu_5] complex (top) and in the three-dimensional network viewed along the *b* axis (labelled in dotted green lines) (bottom).

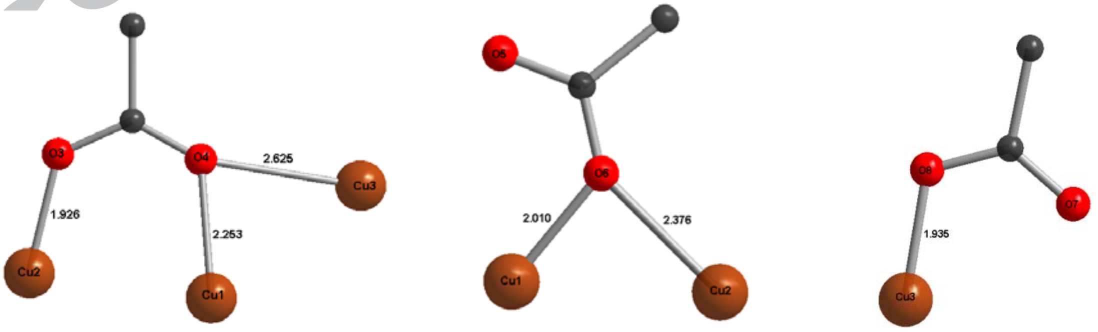

Figure S7. Different coordinating modes of the acetate ligands in **1**.

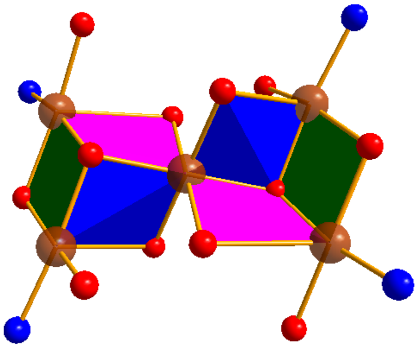

Figure S8. Vertex shared dicubane structure showing three colored (blue, green and pink) tetragonal faces of two partial cubanes.

[1] W. T. Pennington, *Applied crystallography*. **1999**. *32*. 1028.

Graphical Abstract

Self-Assembly of a Pentanuclear {Cu_5} Complex Resulting from the Trapping of a Cu^{2+} Ion by Two {Cu_2} Building Units

Aloke Kumar Ghosh, Rodolphe Clérac, Corine Mathonière and Debashis Ray*

The binding of acetate anions in three different modes along with water derived μ_3-hydroxido groups dictate the stabilization of a pentanuclear copper(II) complex resulting from the self-assembly of two dinuclear {Cu_2} units around a central copper ion.

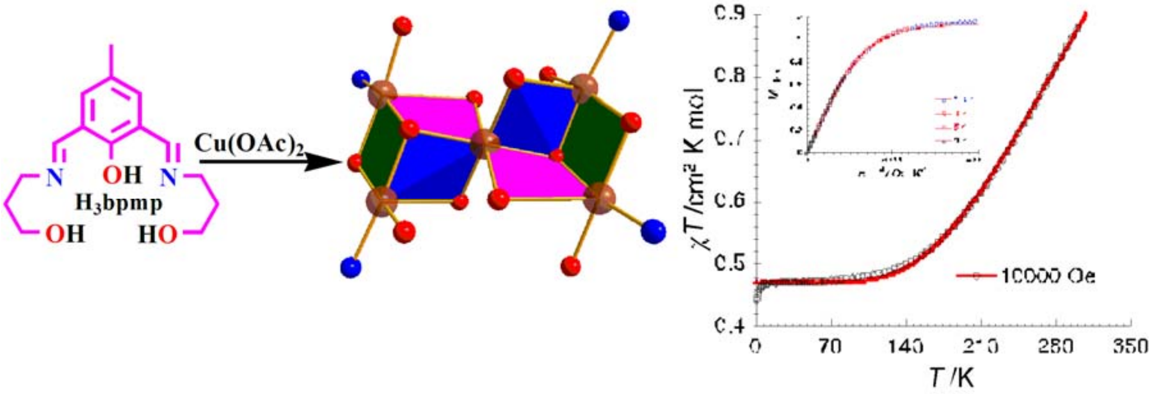

```
data_publication_text
_publ_requested_journal         Polyhedron
_publ_contact_author_name       "'Prof. Debashis Ray'"
_publ_contact_author_address
;Prof. Debashis Ray
 Department of Chemistry
 Indian Institute of Technology
 Kharagpur-721302
 India
;
_publ_contact_author_email      dray@chem.iitkgp.ernet.in
_publ_contact_author_phone      03222-283324
_publ_contact_author_fax        03222-255303
loop_
_publ_author_name
_publ_author_address
"'Prof. Debashis Ray', Aloke Kumar Ghosh"
;Prof. Debashis Ray
 Department of Chemistry
 Indian Institute of Technology
 Kharagpur-721302
 India
;
```

```

data_platon

_audit_creation_method           SHELXL-97
_chemical_name_systematic
;
 ?
;
_chemical_name_common            ?
_chemical_melting_point          ?
_chemical_formula_moiety         'C42 H62 Cu5 N4 O20, 2(H2 O)'
_chemical_formula_sum
 'C42 H66 Cu5 N4 O22'
_chemical_formula_weight         1296.74

loop_
 _atom_type_symbol
 _atom_type_description
 _atom_type_scat_dispersion_real
 _atom_type_scat_dispersion_imag
 _atom_type_scat_source
 'C'  'C'   0.0030   0.0020
 'International Tables Vol C Tables 4.2.6.8 and 6.1.1.4'
 'H'  'H'   0.0000   0.0000
 'International Tables Vol C Tables 4.2.6.8 and 6.1.1.4'
```

```
 'Cu'  'Cu'   0.3200   1.2650
 'International Tables Vol C Tables 4.2.6.8 and 6.1.1.4'
 'N'  'N'   0.0060   0.0030
 'International Tables Vol C Tables 4.2.6.8 and 6.1.1.4'
 'O'  'O'   0.0110   0.0060
 'International Tables Vol C Tables 4.2.6.8 and 6.1.1.4'

_symmetry_cell_setting            'Monoclinic'
_symmetry_space_group_name_H-M    'P 21/c'

loop_
 _symmetry_equiv_pos_as_xyz
 'x, y, z'
 '-x, y+1/2, -z+1/2'
 '-x, -y, -z'
 'x, -y-1/2, z-1/2'

_cell_length_a                    11.4604(7)
_cell_length_b                    13.7598(8)
_cell_length_c                    17.3334(10)
_cell_angle_alpha                 90.00
_cell_angle_beta                  103.317(2)
_cell_angle_gamma                 90.00
_cell_volume                      2659.9(3)
_cell_formula_units_Z             2
```

```
_cell_measurement_temperature    293(2)
_cell_measurement_reflns_used    ?
_cell_measurement_theta_min      ?
_cell_measurement_theta_max      ?

_exptl_crystal_description       'block'
_exptl_crystal_colour            'green'
_exptl_crystal_size_max          0.36
_exptl_crystal_size_mid          0.25
_exptl_crystal_size_min          0.15
_exptl_crystal_density_meas      ?
_exptl_crystal_density_diffrn    1.618
_exptl_crystal_density_method    'not measured'
_exptl_crystal_F_000             1334
_exptl_absorpt_coefficient_mu    2.047
_exptl_absorpt_correction_type   'empirical'
_exptl_absorpt_correction_T_min  0.547
_exptl_absorpt_correction_T_max  0.736
_exptl_absorpt_process_details   ?

_exptl_special_details
;
 ?
;

```

```
_diffrn_ambient_temperature      293(2)
_diffrn_radiation_wavelength     0.71073
_diffrn_radiation_type           MoK\a
_diffrn_radiation_source         'fine-focus sealed tube'
_diffrn_radiation_monochromator  graphite
_diffrn_measurement_device_type  ?
_diffrn_measurement_method       ?
_diffrn_detector_area_resol_mean ?
_diffrn_standards_number         ?
_diffrn_standards_interval_count ?
_diffrn_standards_interval_time  ?
_diffrn_standards_decay_%        ?
_diffrn_reflns_number            39472
_diffrn_reflns_av_R_equivalents  0.0377
_diffrn_reflns_av_sigmaI/netI    0.0374
_diffrn_reflns_limit_h_min       -16
_diffrn_reflns_limit_h_max       16
_diffrn_reflns_limit_k_min       -19
_diffrn_reflns_limit_k_max       20
_diffrn_reflns_limit_l_min       -23
_diffrn_reflns_limit_l_max       22
_diffrn_reflns_theta_min         1.83
_diffrn_reflns_theta_max         31.86
_reflns_number_total             8976
_reflns_number_gt                5671
```

```
_reflns_threshold_expression     >2\s(I)

_computing_data_collection       'Bruker'
_computing_cell_refinement       'Bruker'
_computing_data_reduction        'Bruker'
_computing_structure_solution     'SHELXL-97 (Sheldrick,1990)'
_computing_structure_refinement   'SHELXL-97 (Sheldrick, 2008)'
_computing_molecular_graphics     'ORTEPIII (Burnett & Johnson, 1996)'
_computing_publication_material
'SHELXL-97 (Sheldrick, 1997), PARST (Nardelli, 1995)'

_refine_special_details
;
 Refinement of F^2^ against ALL reflections.  The weighted R-factor wR and
 goodness of fit S are based on F^2^, conventional R-factors R are based
 on F, with F set to zero for negative F^2^. The threshold expression of
 F^2^ > 2\s(F^2^) is used only for calculating R-factors(gt) etc. and is
 not relevant to the choice of reflections for refinement.  R-factors based
 on F^2^ are statistically about twice as large as those based on F, and R-
 factors based on ALL data will be even larger.
;

_refine_ls_structure_factor_coef  Fsqd
_refine_ls_matrix_type           full
_refine_ls_weighting_scheme       calc
```

```
_refine_ls_weighting_details
 'calc w=1/[\s^2^(Fo^2^)+(0.0100P)^2^+0.0000P] where P=(Fo^2^+2Fc^2^)/3'
_atom_sites_solution_primary      direct
_atom_sites_solution_secondary    difmap
_atom_sites_solution_hydrogens    geom
_refine_ls_hydrogen_treatment     mixed
_refine_ls_extinction_method      none
_refine_ls_extinction_coef        ?
_refine_ls_number_reflns          8976
_refine_ls_number_parameters      335
_refine_ls_number_restraints      0
_refine_ls_R_factor_all           0.0657
_refine_ls_R_factor_gt            0.0389
_refine_ls_wR_factor_ref          0.0702
_refine_ls_wR_factor_gt           0.0680
_refine_ls_goodness_of_fit_ref    1.899
_refine_ls_restrained_S_all       1.899
_refine_ls_shift/su_max           0.009
_refine_ls_shift/su_mean          0.004

loop_
 _atom_site_label
 _atom_site_type_symbol
 _atom_site_fract_x
 _atom_site_fract_y
```

```
_atom_site_fract_z
_atom_site_U_iso_or_equiv
_atom_site_adp_type
_atom_site_occupancy
_atom_site_symmetry_multiplicity
_atom_site_calc_flag
_atom_site_refinement_flags
_atom_site_disorder_assembly
_atom_site_disorder_group
Cu1 Cu 1.0000 0.5000 0.0000 0.02933(10) Uani 1 2 d S . .
Cu2 Cu 0.75750(2) 0.575931(18) 0.000078(15) 0.02897(8) Uani 1 1 d . . .
Cu3 Cu 0.76993(2) 0.362706(19) -0.047247(16) 0.03286(8) Uani 1 1 d . . .
O1 O 0.69148(12) 0.44779(10) 0.01807(9) 0.0312(3) Uani 1 1 d . . .
O2 O 0.83217(12) 0.48999(9) -0.06229(8) 0.0288(3) Uani 1 1 d . . .
H2' H 0.8373 0.5010 -0.1017 0.043 Uiso 1 1 d R . .
O3 O 0.81144(13) 0.69178(10) -0.04366(9) 0.0386(4) Uani 1 1 d . . .
O4 O 1.00597(14) 0.65893(11) -0.02977(10) 0.0430(4) Uani 1 1 d . . .
O5 O 1.08239(14) 0.47165(12) 0.19000(9) 0.0410(4) Uani 1 1 d . . .
O6 O 0.93210(13) 0.52706(11) 0.09460(9) 0.0347(4) Uani 1 1 d . . .
O7 O 0.67604(16) 0.35929(13) -0.21318(11) 0.0570(5) Uani 1 1 d . . .
O8 O 0.83454(14) 0.30123(11) -0.12873(10) 0.0406(4) Uani 1 1 d . . .
O9 O 0.6561(2) -0.05496(14) -0.08274(15) 0.0955(8) Uani 1 1 d . . .
H9 H 0.5835 -0.0524 -0.0864 0.143 Uiso 1 1 d R . .
O10 O 0.79895(16) 0.94338(12) 0.15349(11) 0.0605(5) Uani 1 1 d . . .
H10' H 0.8351 0.9437 0.1929 0.091 Uiso 1 1 d R . .
```

```
N1 N 0.67036(15) 0.64316(12) 0.06866(11) 0.0301(4) Uani 1 1 d . . .
N2 N 0.70447(17) 0.24651(13) -0.00979(11) 0.0390(5) Uani 1 1 d . . .
C1 C 0.3784(2) 0.34752(19) 0.21636(15) 0.0526(7) Uani 1 1 d . . .
H1A H 0.3460 0.4052 0.2345 0.079 Uiso 1 1 calc R . .
H1B H 0.4230 0.3118 0.2611 0.079 Uiso 1 1 calc R . .
H1C H 0.3142 0.3079 0.1873 0.079 Uiso 1 1 calc R . .
C2 C 0.46046(19) 0.37523(18) 0.16314(13) 0.0382(6) Uani 1 1 d . . .
C3 C 0.50892(19) 0.30543(17) 0.12271(13) 0.0375(6) Uani 1 1 d . . .
H3 H 0.4889 0.2407 0.1282 0.045 Uiso 1 1 calc R . .
C4 C 0.58697(19) 0.32763(16) 0.07379(13) 0.0326(5) Uani 1 1 d . . .
C5 C 0.61872(17) 0.42559(15) 0.06496(12) 0.0282(5) Uani 1 1 d . . .
C6 C 0.57060(18) 0.49777(15) 0.10617(13) 0.0301(5) Uani 1 1 d . . .
C7 C 0.49174(19) 0.47030(17) 0.15337(13) 0.0367(6) Uani 1 1 d . . .
H7 H 0.4590 0.5187 0.1793 0.044 Uiso 1 1 calc R . .
C8 C 0.59865(18) 0.60099(16) 0.10475(13) 0.0339(5) Uani 1 1 d . . .
H8 H 0.5595 0.6413 0.1337 0.041 Uiso 1 1 calc R . .
C9 C 0.68939(19) 0.74858(15) 0.07957(14) 0.0373(6) Uani 1 1 d . . .
H9A H 0.6319 0.7750 0.1072 0.045 Uiso 1 1 calc R . .
H9B H 0.6766 0.7800 0.0282 0.045 Uiso 1 1 calc R . .
C10 C 0.8162(2) 0.76943(16) 0.12698(14) 0.0440(6) Uani 1 1 d . . .
H10A H 0.8199 0.7580 0.1827 0.053 Uiso 1 1 calc R . .
H10B H 0.8711 0.7244 0.1106 0.053 Uiso 1 1 calc R . .
C11 C 0.8571(2) 0.87272(19) 0.11665(16) 0.0539(7) Uani 1 1 d . . .
H11A H 0.9428 0.8770 0.1385 0.065 Uiso 1 1 calc R . .
H11B H 0.8424 0.8871 0.0605 0.065 Uiso 1 1 calc R . .
```

```
C12 C 0.6331(2) 0.24623(16) 0.03720(14) 0.0392(6) Uani 1 1 d . . .
H12 H 0.6074 0.1853 0.0495 0.047 Uiso 1 1 calc R . .
C13 C 0.7408(2) 0.14913(17) -0.03494(15) 0.0461(6) Uani 1 1 d . . .
H13A H 0.7403 0.1019 0.0066 0.055 Uiso 1 1 calc R . .
H13B H 0.8218 0.1528 -0.0429 0.055 Uiso 1 1 calc R . .
C14 C 0.6575(2) 0.11672(19) -0.10992(17) 0.0574(7) Uani 1 1 d . . .
H14A H 0.6634 0.1607 -0.1526 0.069 Uiso 1 1 calc R . .
H14B H 0.5756 0.1187 -0.1035 0.069 Uiso 1 1 calc R . .
C15 C 0.6878(3) 0.0129(2) -0.1316(2) 0.0773(10) Uani 1 1 d . . .
H15A H 0.6463 -0.0007 -0.1859 0.093 Uiso 1 1 calc R . .
H15B H 0.7733 0.0083 -0.1284 0.093 Uiso 1 1 calc R . .
C16 C 0.9162(2) 0.70953(16) -0.05335(13) 0.0353(5) Uani 1 1 d . . .
C17 C 0.9261(2) 0.8010(2) -0.09942(18) 0.0688(9) Uani 1 1 d . . .
H17A H 0.8544 0.8389 -0.1044 0.103 Uiso 1 1 calc R . .
H17B H 0.9364 0.7841 -0.1512 0.103 Uiso 1 1 calc R . .
H17C H 0.9939 0.8382 -0.0720 0.103 Uiso 1 1 calc R . .
C18 C 0.9780(2) 0.50250(16) 0.16615(14) 0.0335(5) Uani 1 1 d . . .
C19 C 0.8990(2) 0.51150(19) 0.22399(15) 0.0516(7) Uani 1 1 d . . .
H19A H 0.8206 0.5327 0.1965 0.077 Uiso 1 1 calc R . .
H19B H 0.9329 0.5580 0.2642 0.077 Uiso 1 1 calc R . .
H19C H 0.8930 0.4495 0.2482 0.077 Uiso 1 1 calc R . .
C20 C 0.7750(2) 0.31889(17) -0.19814(16) 0.0406(6) Uani 1 1 d . . .
C21 C 0.8310(2) 0.2868(2) -0.26475(15) 0.0602(8) Uani 1 1 d . . .
H21A H 0.9134 0.2699 -0.2436 0.090 Uiso 1 1 calc R . .
H21B H 0.8265 0.3388 -0.3022 0.090 Uiso 1 1 calc R . .
```

```
H21C H 0.7886 0.2312 -0.2907 0.090 Uiso 1 1 calc R . .
O11 O 0.59048(17) 0.05364(14) 0.14169(12) 0.0712(6) Uani 1 1 d . . .
H11' H 0.6396 0.0146 0.1222 0.107 Uiso 1 1 d R . .
H11" H 0.6322 0.0923 0.1978 0.107 Uiso 1 1 d R . .

loop_
 _atom_site_aniso_label
 _atom_site_aniso_U_11
 _atom_site_aniso_U_22
 _atom_site_aniso_U_33
 _atom_site_aniso_U_23
 _atom_site_aniso_U_13
 _atom_site_aniso_U_12
Cu1 0.02490(19) 0.0394(2) 0.0241(2) -0.00031(17) 0.00643(16) 0.00325(16)
Cu2 0.02994(14) 0.02809(14) 0.03146(17) -0.00061(12) 0.01236(12) 0.00206(11)
Cu3 0.04019(17) 0.02926(14) 0.03255(17) -0.00336(12) 0.01540(13) -0.00062(12)
O1 0.0335(8) 0.0288(8) 0.0363(9) -0.0015(7) 0.0183(7) -0.0014(6)
O2 0.0332(8) 0.0323(8) 0.0232(8) -0.0015(6) 0.0112(6) 0.0001(6)
O3 0.0424(9) 0.0303(8) 0.0469(11) 0.0040(7) 0.0184(8) 0.0006(7)
O4 0.0383(9) 0.0446(10) 0.0449(11) 0.0052(8) 0.0069(8) -0.0012(8)
O5 0.0341(9) 0.0615(11) 0.0276(9) 0.0084(8) 0.0074(7) 0.0101(8)
O6 0.0313(8) 0.0481(10) 0.0251(9) 0.0039(7) 0.0074(7) 0.0090(7)
O7 0.0497(11) 0.0666(12) 0.0553(12) -0.0060(10) 0.0131(9) 0.0147(10)
O8 0.0497(10) 0.0415(9) 0.0332(10) -0.0064(8) 0.0145(8) 0.0020(8)
O9 0.1015(18) 0.0461(13) 0.126(2) 0.0070(13) 0.0000(16) -0.0007(12)
```

O10	0.0748(13)	0.0503(11)	0.0490(12)	-0.0158(9)	-0.0011(10)	0.0036(9)
N1	0.0290(10)	0.0293(9)	0.0327(11)	-0.0012(8)	0.0082(8)	0.0055(8)
N2	0.0489(12)	0.0298(10)	0.0416(13)	-0.0036(9)	0.0174(10)	-0.0018(9)
C1	0.0489(16)	0.0721(19)	0.0423(17)	0.0070(14)	0.0220(13)	-0.0058(13)
C2	0.0311(13)	0.0552(15)	0.0298(14)	0.0071(12)	0.0103(10)	-0.0016(11)
C3	0.0383(13)	0.0402(13)	0.0351(14)	0.0069(11)	0.0107(11)	-0.0060(11)
C4	0.0333(12)	0.0354(12)	0.0294(13)	0.0042(10)	0.0078(10)	0.0005(10)
C5	0.0227(11)	0.0373(12)	0.0244(12)	0.0016(10)	0.0046(9)	-0.0001(9)
C6	0.0258(11)	0.0364(12)	0.0286(13)	0.0003(10)	0.0073(9)	0.0032(9)
C7	0.0314(12)	0.0487(14)	0.0319(14)	-0.0014(11)	0.0114(11)	0.0057(10)
C8	0.0292(12)	0.0389(13)	0.0352(14)	-0.0060(10)	0.0106(10)	0.0077(10)
C9	0.0411(14)	0.0312(12)	0.0418(15)	-0.0067(11)	0.0139(12)	0.0037(10)
C10	0.0516(15)	0.0420(14)	0.0367(15)	-0.0107(11)	0.0068(12)	-0.0015(11)
C11	0.0583(17)	0.0573(17)	0.0479(18)	-0.0187(14)	0.0158(14)	-0.0158(14)
C12	0.0471(14)	0.0307(12)	0.0418(15)	0.0025(11)	0.0140(12)	-0.0060(10)
C13	0.0512(16)	0.0390(14)	0.0496(17)	-0.0013(12)	0.0149(13)	-0.0010(11)
C14	0.0565(17)	0.0501(17)	0.063(2)	-0.0008(14)	0.0085(15)	-0.0094(13)
C15	0.087(2)	0.060(2)	0.092(3)	-0.0213(19)	0.035(2)	-0.0002(17)
C16	0.0444(14)	0.0346(12)	0.0280(14)	-0.0026(10)	0.0107(11)	-0.0049(11)
C17	0.0640(19)	0.0594(19)	0.090(2)	0.0325(17)	0.0330(18)	-0.0015(15)
C18	0.0346(13)	0.0362(12)	0.0314(14)	-0.0007(11)	0.0112(11)	-0.0006(10)
C19	0.0481(15)	0.0734(19)	0.0383(16)	0.0095(14)	0.0199(13)	0.0137(13)
C20	0.0454(15)	0.0373(13)	0.0423(17)	-0.0103(12)	0.0165(13)	-0.0050(11)
C21	0.0650(18)	0.074(2)	0.0439(17)	-0.0142(15)	0.0180(14)	0.0118(15)
O11	0.0701(13)	0.0639(13)	0.0731(15)	0.0055(11)	0.0033(11)	-0.0043(10)

```
_geom_special_details
;
 All s.u.'s (except the s.u. in the dihedral angle between two l.s. planes)
 are estimated using the full covariance matrix.  The cell s.u.'s are taken
 into account individually in the estimation of s.u.'s in distances, angles
 and torsion angles; correlations between s.u.'s in cell parameters are only
 used when they are defined by crystal symmetry.  An approximate (isotropic)
 treatment of cell s.u.'s is used for estimating s.u.'s involving l.s. planes.
;

loop_
 _geom_bond_atom_site_label_1
 _geom_bond_atom_site_label_2
 _geom_bond_distance
 _geom_bond_site_symmetry_2
 _geom_bond_publ_flag
Cu1 O2 1.9818(13) 3_765 ?
Cu1 O2 1.9818(13) . ?
Cu1 O6 2.0051(14) . ?
Cu1 O6 2.0051(14) 3_765 ?
Cu1 O4 2.2516(15) 3_765 ?
Cu1 O4 2.2516(15) . ?
Cu1 Cu2 2.9694(3) 3_765 ?
Cu1 Cu2 2.9694(3) . ?
```

Cu1 Cu3 3.1933(3) 3_765 ?
Cu1 Cu3 3.1933(3) . ?
Cu1 H2' 2.2518 . ?
Cu2 O3 1.9271(14) . ?
Cu2 O2 1.9302(13) . ?
Cu2 N1 1.9527(17) . ?
Cu2 O1 1.9716(14) . ?
Cu2 O6 2.3728(15) . ?
Cu2 Cu3 3.0586(4) . ?
Cu3 O2 1.9314(13) . ?
Cu3 O8 1.9340(15) . ?
Cu3 N2 1.9403(18) . ?
Cu3 O1 1.9823(14) . ?
Cu3 O4 2.6244(16) 3_765 ?
Cu3 C20 2.698(2) . ?
Cu3 H2' 2.3337 . ?
O1 C5 1.327(2) . ?
O2 H2' 0.7155 . ?
O3 C16 1.274(2) . ?
O4 C16 1.232(3) . ?
O4 Cu3 2.6244(16) 3_765 ?
O5 C18 1.247(2) . ?
O6 C18 1.276(3) . ?
O7 C20 1.235(3) . ?
O8 C20 1.263(3) . ?

```
O9 C15 1.366(4) . ?
O9 H9 0.8200 . ?
O10 C11 1.411(3) . ?
O10 H10' 0.7125 . ?
N1 C8 1.281(3) . ?
N1 C9 1.473(3) . ?
N2 C12 1.280(3) . ?
N2 C13 1.498(3) . ?
C1 C2 1.510(3) . ?
C1 H1A 0.9600 . ?
C1 H1B 0.9600 . ?
C1 H1C 0.9600 . ?
C2 C3 1.379(3) . ?
C2 C7 1.377(3) . ?
C3 C4 1.401(3) . ?
C3 H3 0.9300 . ?
C4 C5 1.414(3) . ?
C4 C12 1.446(3) . ?
C5 C6 1.408(3) . ?
C6 C7 1.403(3) . ?
C6 C8 1.458(3) . ?
C7 H7 0.9300 . ?
C8 H8 0.9300 . ?
C9 C10 1.523(3) . ?
C9 H9A 0.9700 . ?
```

C9 H9B 0.9700 . ?
C10 C11 1.520(3) . ?
C10 H10A 0.9700 . ?
C10 H10B 0.9700 . ?
C11 H11A 0.9700 . ?
C11 H11B 0.9700 . ?
C12 H12 0.9300 . ?
C13 C14 1.493(3) . ?
C13 H13A 0.9700 . ?
C13 H13B 0.9700 . ?
C14 C15 1.537(4) . ?
C14 H14A 0.9700 . ?
C14 H14B 0.9700 . ?
C15 H15A 0.9700 . ?
C15 H15B 0.9700 . ?
C16 C17 1.509(3) . ?
C17 H17A 0.9601 . ?
C17 H17B 0.9601 . ?
C17 H17C 0.9601 . ?
C18 C19 1.503(3) . ?
C19 H19A 0.9600 . ?
C19 H19B 0.9600 . ?
C19 H19C 0.9600 . ?
C20 C21 1.511(3) . ?
C21 H21A 0.9600 . ?

```
C21 H21B 0.9600 . ?
C21 H21C 0.9600 . ?
O11 H11' 0.8991 . ?
O11 H11" 1.1154 . ?

loop_
 _geom_angle_atom_site_label_1
 _geom_angle_atom_site_label_2
 _geom_angle_atom_site_label_3
 _geom_angle
 _geom_angle_site_symmetry_1
 _geom_angle_site_symmetry_3
 _geom_angle_publ_flag
O2 Cu1 O2 180.00(7) 3_765 . ?
O2 Cu1 O6 93.00(6) 3_765 . ?
O2 Cu1 O6 87.00(6) . . ?
O2 Cu1 O6 87.00(6) 3_765 3_765 ?
O2 Cu1 O6 93.00(6) . 3_765 ?
O6 Cu1 O6 180.0 . 3_765 ?
O2 Cu1 O4 91.12(5) 3_765 3_765 ?
O2 Cu1 O4 88.88(5) . 3_765 ?
O6 Cu1 O4 87.42(6) . 3_765 ?
O6 Cu1 O4 92.58(6) 3_765 3_765 ?
O2 Cu1 O4 88.88(5) 3_765 . ?
O2 Cu1 O4 91.12(5) . . ?
```

```
O6 Cu1 O4 92.58(6) . . ?
O6 Cu1 O4 87.42(6) 3_765 . ?
O4 Cu1 O4 180.000(1) 3_765 . ?
O2 Cu1 Cu2 39.98(4) 3_765 3_765 ?
O2 Cu1 Cu2 140.02(4) . 3_765 ?
O6 Cu1 Cu2 127.25(4) . 3_765 ?
O6 Cu1 Cu2 52.75(4) 3_765 3_765 ?
O4 Cu1 Cu2 74.71(4) 3_765 3_765 ?
O4 Cu1 Cu2 105.29(4) . 3_765 ?
O2 Cu1 Cu2 140.02(4) 3_765 . ?
O2 Cu1 Cu2 39.98(4) . . ?
O6 Cu1 Cu2 52.75(4) . . ?
O6 Cu1 Cu2 127.25(4) 3_765 . ?
O4 Cu1 Cu2 105.29(4) 3_765 . ?
O4 Cu1 Cu2 74.71(4) . . ?
Cu2 Cu1 Cu2 180.0 3_765 . ?
O2 Cu1 Cu3 34.79(4) 3_765 3_765 ?
O2 Cu1 Cu3 145.21(4) . 3_765 ?
O6 Cu1 Cu3 97.67(4) . 3_765 ?
O6 Cu1 Cu3 82.33(4) 3_765 3_765 ?
O4 Cu1 Cu3 125.64(4) 3_765 3_765 ?
O4 Cu1 Cu3 54.36(4) . 3_765 ?
Cu2 Cu1 Cu3 59.380(8) 3_765 3_765 ?
Cu2 Cu1 Cu3 120.620(8) . 3_765 ?
O2 Cu1 Cu3 145.21(4) 3_765 . ?
```

```
O2 Cu1 Cu3 34.79(4) . . ?
O6 Cu1 Cu3 82.33(4) . . ?
O6 Cu1 Cu3 97.67(4) 3_765 . ?
O4 Cu1 Cu3 54.36(4) 3_765 . ?
O4 Cu1 Cu3 125.64(4) . . ?
Cu2 Cu1 Cu3 120.620(8) 3_765 . ?
Cu2 Cu1 Cu3 59.380(8) . . ?
Cu3 Cu1 Cu3 180.0 3_765 . ?
O2 Cu1 H2' 162.0 3_765 . ?
O2 Cu1 H2' 18.0 . . ?
O6 Cu1 H2' 103.4 . . ?
O6 Cu1 H2' 76.6 3_765 . ?
O4 Cu1 H2' 97.0 3_765 . ?
O4 Cu1 H2' 83.0 . . ?
Cu2 Cu1 H2' 127.5 3_765 . ?
Cu2 Cu1 H2' 52.5 . . ?
Cu3 Cu1 H2' 133.1 3_765 . ?
Cu3 Cu1 H2' 46.9 . . ?
O3 Cu2 O2 93.59(6) . . ?
O3 Cu2 N1 95.91(7) . . ?
O2 Cu2 N1 170.43(7) . . ?
O3 Cu2 O1 166.29(6) . . ?
O2 Cu2 O1 77.09(5) . . ?
N1 Cu2 O1 93.36(6) . . ?
O3 Cu2 O6 102.13(6) . . ?
```

```
O2 Cu2 O6 78.52(5) . . ?
N1 Cu2 O6 100.49(6) . . ?
O1 Cu2 O6 86.02(6) . . ?
O3 Cu2 Cu1 84.59(4) . . ?
O2 Cu2 Cu1 41.27(4) . . ?
N1 Cu2 Cu1 140.98(5) . . ?
O1 Cu2 Cu1 94.52(4) . . ?
O6 Cu2 Cu1 42.27(3) . . ?
O3 Cu2 Cu3 130.46(5) . . ?
O2 Cu2 Cu3 37.64(4) . . ?
N1 Cu2 Cu3 132.81(5) . . ?
O1 Cu2 Cu3 39.45(4) . . ?
O6 Cu2 Cu3 80.18(4) . . ?
Cu1 Cu2 Cu3 63.957(7) . . ?
O2 Cu3 O8 94.74(6) . . ?
O2 Cu3 N2 167.35(7) . . ?
O8 Cu3 N2 97.27(7) . . ?
O2 Cu3 O1 76.81(5) . . ?
O8 Cu3 O1 167.34(7) . . ?
N2 Cu3 O1 91.97(7) . . ?
O2 Cu3 O4 79.80(5) . 3_765 ?
O8 Cu3 O4 80.06(6) . 3_765 ?
N2 Cu3 O4 98.33(7) . 3_765 ?
O1 Cu3 O4 107.21(6) . 3_765 ?
O2 Cu3 C20 88.89(6) . . ?
```

```
O8 Cu3 C20 25.43(7) . . ?
N2 Cu3 C20 103.68(7) . . ?
O1 Cu3 C20 143.09(7) . . ?
O4 Cu3 C20 103.34(7) 3_765 . ?
O2 Cu3 Cu2 37.61(4) . . ?
O8 Cu3 Cu2 131.66(5) . . ?
N2 Cu3 Cu2 130.93(6) . . ?
O1 Cu3 Cu2 39.20(4) . . ?
O4 Cu3 Cu2 94.19(4) 3_765 . ?
C20 Cu3 Cu2 119.15(5) . . ?
O2 Cu3 Cu1 35.84(4) . . ?
O8 Cu3 Cu1 90.78(5) . . ?
N2 Cu3 Cu1 139.61(6) . . ?
O1 Cu3 Cu1 87.73(4) . . ?
O4 Cu3 Cu1 44.21(3) 3_765 . ?
C20 Cu3 Cu1 100.37(5) . . ?
Cu2 Cu3 Cu1 56.664(7) . . ?
O2 Cu3 H2' 16.0 . . ?
O8 Cu3 H2' 81.0 . . ?
N2 Cu3 H2' 175.5 . . ?
O1 Cu3 H2' 89.2 . . ?
O4 Cu3 H2' 85.5 3_765 . ?
C20 Cu3 H2' 73.0 . . ?
Cu2 Cu3 H2' 50.7 . . ?
Cu1 Cu3 H2' 44.8 . . ?
```

C5 O1 Cu2 128.38(13) . . ?

C5 O1 Cu3 130.20(13) . . ?

Cu2 O1 Cu3 101.35(6) . . ?

Cu3 O2 Cu2 104.75(6) . . ?

Cu3 O2 Cu1 109.37(6) . . ?

Cu2 O2 Cu1 98.75(6) . . ?

Cu3 O2 H2' 115.8 . . ?

Cu2 O2 H2' 123.3 . . ?

Cu1 O2 H2' 102.9 . . ?

C16 O3 Cu2 127.45(14) . . ?

C16 O4 Cu1 123.91(14) . . ?

C16 O4 Cu3 151.39(15) . 3_765 ?

Cu1 O4 Cu3 81.44(5) . 3_765 ?

C18 O6 Cu1 126.49(13) . . ?

C18 O6 Cu2 147.08(14) . . ?

Cu1 O6 Cu2 84.98(5) . . ?

C20 O8 Cu3 113.44(14) . . ?

C15 O9 H9 109.4 . . ?

C11 O10 H10' 101.9 . . ?

C8 N1 C9 118.44(18) . . ?

C8 N1 Cu2 123.95(15) . . ?

C9 N1 Cu2 117.61(14) . . ?

C12 N2 C13 116.34(19) . . ?

C12 N2 Cu3 124.63(15) . . ?

C13 N2 Cu3 119.01(15) . . ?

```
C2 C1 H1A 109.5 . . ?
C2 C1 H1B 109.5 . . ?
H1A C1 H1B 109.5 . . ?
C2 C1 H1C 109.5 . . ?
H1A C1 H1C 109.5 . . ?
H1B C1 H1C 109.5 . . ?
C3 C2 C7 116.9(2) . . ?
C3 C2 C1 121.0(2) . . ?
C7 C2 C1 122.1(2) . . ?
C2 C3 C4 122.9(2) . . ?
C2 C3 H3 118.5 . . ?
C4 C3 H3 118.5 . . ?
C3 C4 C5 119.3(2) . . ?
C3 C4 C12 116.5(2) . . ?
C5 C4 C12 124.18(19) . . ?
O1 C5 C6 121.54(19) . . ?
O1 C5 C4 119.96(19) . . ?
C6 C5 C4 118.50(19) . . ?
C7 C6 C5 119.1(2) . . ?
C7 C6 C8 116.51(19) . . ?
C5 C6 C8 124.41(19) . . ?
C2 C7 C6 123.3(2) . . ?
C2 C7 H7 118.4 . . ?
C6 C7 H7 118.4 . . ?
N1 C8 C6 128.2(2) . . ?
```

N1 C8 H8 115.9 . . ?

C6 C8 H8 115.9 . . ?

N1 C9 C10 110.46(17) . . ?

N1 C9 H9A 109.6 . . ?

C10 C9 H9A 109.6 . . ?

N1 C9 H9B 109.6 . . ?

C10 C9 H9B 109.6 . . ?

H9A C9 H9B 108.1 . . ?

C11 C10 C9 113.2(2) . . ?

C11 C10 H10A 108.9 . . ?

C9 C10 H10A 108.9 . . ?

C11 C10 H10B 108.9 . . ?

C9 C10 H10B 108.9 . . ?

H10A C10 H10B 107.8 . . ?

O10 C11 C10 113.6(2) . . ?

O10 C11 H11A 108.8 . . ?

C10 C11 H11A 108.9 . . ?

O10 C11 H11B 108.8 . . ?

C10 C11 H11B 108.8 . . ?

H11A C11 H11B 107.7 . . ?

N2 C12 C4 128.9(2) . . ?

N2 C12 H12 115.5 . . ?

C4 C12 H12 115.5 . . ?

N2 C13 C14 110.8(2) . . ?

N2 C13 H13A 109.5 . . ?

```
C14 C13 H13A 109.5 . . ?
N2 C13 H13B 109.5 . . ?
C14 C13 H13B 109.5 . . ?
H13A C13 H13B 108.1 . . ?
C13 C14 C15 110.8(2) . . ?
C13 C14 H14A 109.5 . . ?
C15 C14 H14A 109.5 . . ?
C13 C14 H14B 109.5 . . ?
C15 C14 H14B 109.5 . . ?
H14A C14 H14B 108.1 . . ?
O9 C15 C14 112.1(3) . . ?
O9 C15 H15A 109.2 . . ?
C14 C15 H15A 109.2 . . ?
O9 C15 H15B 109.2 . . ?
C14 C15 H15B 109.2 . . ?
H15A C15 H15B 107.9 . . ?
O4 C16 O3 126.1(2) . . ?
O4 C16 C17 119.2(2) . . ?
O3 C16 C17 114.7(2) . . ?
C16 C17 H17A 109.5 . . ?
C16 C17 H17B 109.5 . . ?
H17A C17 H17B 109.5 . . ?
C16 C17 H17C 109.5 . . ?
H17A C17 H17C 109.5 . . ?
H17B C17 H17C 109.5 . . ?
```

```
O5 C18 O6 124.2(2) . . ?
O5 C18 C19 119.1(2) . . ?
O6 C18 C19 116.7(2) . . ?
C18 C19 H19A 109.5 . . ?
C18 C19 H19B 109.5 . . ?
H19A C19 H19B 109.5 . . ?
C18 C19 H19C 109.5 . . ?
H19A C19 H19C 109.5 . . ?
H19B C19 H19C 109.5 . . ?
O7 C20 O8 123.8(2) . . ?
O7 C20 C21 120.1(2) . . ?
O8 C20 C21 116.1(2) . . ?
O7 C20 Cu3 83.13(15) . . ?
O8 C20 Cu3 41.13(10) . . ?
C21 C20 Cu3 156.09(19) . . ?
C20 C21 H21A 109.5 . . ?
C20 C21 H21B 109.5 . . ?
H21A C21 H21B 109.5 . . ?
C20 C21 H21C 109.5 . . ?
H21A C21 H21C 109.5 . . ?
H21B C21 H21C 109.5 . . ?
H11' O11 H11" 115.7 . . ?

_diffrn_measured_fraction_theta_max    0.983
_diffrn_reflns_theta_full              31.86
```

```
_diffrn_measured_fraction_theta_full   0.983
_refine_diff_density_max    0.597
_refine_diff_density_min   -0.629
_refine_diff_density_rms    0.093
```